Mechanisms supporting long propagation regimes of photorefractive solitons

Eugenio DelRe,[1,2,*] Angelo D'Ercole,[1,3] and Elia Palange[3,4]
[1]*Dipartimento di Fisica, Università dell'Aquila, 67010 L'Aquila, Italy*
[2]*Istituto Nazionale Fisica della Materia, Unità di Roma "La Sapienza," 00185 Rome, Italy*
[3]*Dipartimento di Ingegneria Elettrica, Università dell'Aquila, 67040 Monteluco di Roio (L'Aquila), Italy*
[4]*Istituto Nazionale Fisica della Materia, Unità dell'Aquila, 67010 L'Aquila, Italy*
(Received 27 May 2004; published 17 March 2005)

We extend investigation of one-dimensional solitons in biased photorefractive crystals to long propagation regimes, where self-trapping over a large number of linear diffraction lengths combines with the progressive growth of generally distortive spatially nonlocal components. Results indicate that saturation halts the radiative misshaping of the soliton, which follows that specific bending trajectory along which its evolution is governed by the same local screening nonlinearity that intervenes in short propagation conditions, where spatial nonlocality has a negligible effect. This finding not only allows the prediction of the curvature and of the relative role of charge displacement and diffusion, but implies a set of interesting observable effects, such as boomerangs, counterpropagating and cavity geometries, quasirectilinear and anomalous collisions, along with specific consequences on soliton arrays and on coupling to bulk gratings.

DOI: 10.1103/PhysRevE.71.036610 PACS number(s): 42.65.Tg, 42.65.Hw, 42.70.Nq

From their discovery more than a decade ago, photorefractive solitons [1] have represented one of the foremost instruments in the study of spatial effects in nonlinear optics, arguably playing—in space—the role that Kerr materials play in time [2]. From the fundamental perspective, we should mention the observation of stable one- and two-dimensional self-trapping in a bulk environment, soliton spiralling [3], incoherent self-trapping [4], soliton arrays [5], and, from the applicative side, optical steering [6], manipulation [7], second-harmonic and parametric oscillation enhancement [8], and soliton electroactivation [9], which forwards considerable functionality compatible with a fast electro-optic response.

In this paper we expand the investigation of solitons to long propagation regimes, where an extended propagation distance L_z and/or a small soliton width Δx imply large values of $\gamma = L_z/L_d$, L_d being the diffraction/nonlinear length [10]. In particular, we are interested in establishing if self-trapped propagation can be observed even in this extreme (if compared to most reported experiments) case, in identifying the underlying physical mechanisms, and, consequently, the possible alterations to the standard experimental design.

The heart of the issue is that in its present understanding, photorefractive self-trapping is believed to be due exclusively to the predominance of the spatially local screening nonlinearity on a nonlocal component due to charge diffusion and displacement [11]. Whereas the first leads to self-lensing and counters diffraction, amounting to a saturated Kerr effect, the second introduces an asymmetric component that, not participating in countering any process, can evidently accumulate in a long propagation and alter the Kerr-saturated picture, to the point of interdicting self-trapping.

The role of nonlocal components in soliton formation was investigated by Carvalho *et al.* [12]. The origin of this more involved response (if compared to Kerr materials) lies in the fact that the nonlinearity is associated to the electro-optic refractive index modulation $\Delta n = -(1/2)n^3 rE$, where r is the relevant electro-optic coefficient, and E the electric field resulting from the spatial redistribution of charges photogenerated by the optical intensity distribution I (space-charge field). The nonlocal effect that stems from charge diffusion is the direct consequence of a spatially dependent I, which translates into a component to $E(I)$ [and $\Delta n(I)$] connected to the gradient of I. The second nonlocal process due to charge displacement (or saturation) is associated to the relationship between the charge density ρ and E, $\rho = \nabla \cdot E/\varepsilon$, for which the dependence of $E(I)$ and hence $\Delta n(I)$ is, in general, integrodifferential. In other words, a localized intensity distribution I, the characteristic soliton trait, renders the local and nonlocal processes *indissoluble*, such that the nonlinearity must be addressed as a whole.

With respect to our present endeavor, the most important result is that when an appropriate soliton-suppoting external field E_0 is applied, the nonlocal component constitutes a correction whose effect self-bends the soliton trajectory through a distortion that accumulates *nonlinearly* along the propagation axis z, according to the scaling $\delta I \propto L_z^2/\Delta x \propto L_z^2/\sqrt{L_d}$ (for a Gaussian-like launch beam) [13]. The effect has been documented in both the one-dimensional and two-dimensional cases [14], and accompanies, to a varied degree, *all* soliton observations.

One theoretical approach is to attempt a prediction based on results for the Raman shift in temporal Kerr solitons [15], where nonlocality (in time) resulting from a delayed response leads to an apparently analogous nonlinear propagation setting [16]. Specializing the nonlocal coupling constant to the photorefractive effect, we find that, contrary to the Raman case (in which distortions can be negligible [16]), behavior depends in a nontrivial manner on the particular soliton parameters. More importantly, predictions corroborate the conclusion that this accumulation fundamentally al-

*Electronic address: eugenio.delre@aquila.infn.it

ters the nature of the nonlinearity. In particular, long propagation regimes should not support localized waves with particlelike properties, and solitons themselves are superseded by Airy waves. This picture, however, is based on conditions in which nonlinearity is unsaturated. This, along with the absence of the correct relationship of the nonlocal coupling constant on the parameters of the soliton, and of a term describing charge displacement, render the Raman-analogous approach ineffective.

Detailed experiments aimed at establishing a quantitative comparison to the local screening nonlinearity have been systematically reported by Kos *et al.* for ferroelectric SBN (strontium-barium-niobate) [17]. The quantitative discrepancy observed in some experimental conditions has been specifically attributed to the coupling of spurious light into the soliton, a consequence of the beam geometry. In particular, a divergence from the model due to the nonlocal component of the response was *excluded* for saturated conditions, since results would converge to predictions of the local model for increasing values of γ (experiments reported for $\gamma=3$ and 7).

Therefore, although no evidence of soliton decay through asymmetric radiation has been reported, and, as indicated by Singh *et al.* [12], the distortion in soliton trajectory is apparently not accompanied by emission, yet the validity of the local screening soliton model appears as a consequence of a limited solitonic manifestation, with low values of γ.

We begin our approach to the long propagation regime by introducing a model tuned to actual experimental conditions, this including at once saturation, charge diffusion, charge displacement, and coupling constants that are correctly dependent on physical parameters (as, for example, in Ref. [12]).

In the reduced one-plus-one-dimensional model, photorefractive nonlinearity is generated by the mutual coupling of the optically driven electrostatic field $E(I)$ and beam propagation, described by the parabolic equation for the slowly varying part $A(x,z)$ of the monochromatic optical field ($I=|A|^2$), through the index pattern $\Delta n(I)$ induced by E. To evaluate $E(I)$, we cast the electrostatic problem in normalized units $Y\equiv E/E_0$, E_0 being the external bias field, $Q\equiv(1+I/I_b)$, I_b being the artificial background illumination, the transverse coordinate $\tilde{\xi}\equiv x/x_q$, where $x_q\equiv(\varepsilon_0\varepsilon_r E_0/N_a q)$ is the saturation scale, N_a the concentration of acceptor impurities, q the electron charge. The electron concentration N, N_a, and the donor concentration N_d obey the hierarchy $N\ll N_a\ll N_d$, and Y must satisfy the formally explicit equation [18]

$$Y=\frac{g}{Q}-a\frac{Q'}{Q}+\frac{g}{Q}Y'+a\frac{Y''}{1+Y'}, \tag{1}$$

where the constant $a\equiv(k_bT/qE_0)/x_q$ is of the order of unity (typically $\sim 2-5$), k_b is the Boltzmann constant, T the crystal temperature, and the constant $g\simeq 1$. Primes represent the derivation $d/d\tilde{\xi}$. For typical micron-sized solitons with intensity full width at half maximum (FWHM) $\Delta x\sim 10$ μm, $x_q\sim 0.1$ μm, and $\eta=x_q/\Delta x\sim 0.01$ is an appropriate smallness parameter. Equation (1) can therefore be iteratively solved to $o(\eta^2)$ as

$$Y=\frac{1}{Q}-a\frac{Q'}{Q}-\frac{Q'}{Q}\left(\frac{1}{Q}\right)^2. \tag{2}$$

The local first term $1/Q$ is the drift component, and leads directly to the saturated nonlinearity $\Delta n\propto 1/(1+I/I_b)$ which is associated to screening self-trapping, neglecting all orders in η. The second and third terms of $o(\eta)$ are, respectively, the diffusion field and the charge displacement field.

The resulting nonlinear propagation equation describing paraxial optical one-dimensional phenomenology is

$$i\frac{\partial w}{\partial\zeta}+\frac{\partial^2 w}{\partial\xi^2}-\frac{w}{1+|w|^2}+\alpha\frac{|w|\partial|w|/\partial\xi}{1+|w|^2}w+\beta\frac{|w|\partial|w|/\partial\xi}{(1+|w|^2)^3}w=0, \tag{3}$$

where the full $o(\eta)$ version from Eq. (2) is considered. The wave is expressed in terms of $w(\xi,\zeta)$, where $A=w\sqrt{I_b}$, $\xi=x/x_0$, and $\zeta=z/z_0$. Here $x_0=1/\sqrt{2k/z_0}$, $z_0=n/(k\Delta n_0)$, $k=2\pi n/\lambda$, and $\Delta n_0=(1/2)n^3 rE_0$, λ being the optical wavelength. The nonlocal parameters are $\alpha=2ax_q/x_0=2k_bT/(qE_0x_0)$ and $\beta=2x_q/x_0$.

Our first goal is to clarify soliton behavior described by Eq. (3) through a numerical investigation by means of the split-step Fourier method (or beam propagation method). To conciliate what appear to be strictly soliton manifestations predicted, for example, in Ref. [12] with Airy-like waves predicted in Ref. [16], we simulated the evolution of a $\Delta x=7$-μm beam in a $L_z=9.6$-mm propagation, corresponding to a long propagation $\gamma\simeq 15$ condition. Crystal response is chosen in close conformity with room temperature ferroelectric SBN, i.e., $\varepsilon_r=10^3$, $N_a=5\times 10^{22}$ m^{-3}, $n=2.5$, $r=200$ pm/V, and $\lambda=0.5$ μm. Results for the transition from unsaturated to saturated conditions are shown in Fig. 1, for increasing values of intensity ratio $u_0^2=I_p/I_b$, where I_p is the peak beam intensity. For low values of u_0 self-trapping does not emerge for any value of external bias E_0 (and hence Δn_0), and considerable nonsoliton effects predicted in Ref. [16] appear [Figs. 1(a) and 1(b)]. However, contrary to what therein stated and in conformity with the studies of Ref. [12], as saturation sets in, a regime which best reflects the greater part of experiments, self-trapping is predicted for a specific external bias of $E_0\simeq 4.2$ kV/cm. Here, as indicated in Fig. 1(c), the localized wave *does not* dissolve through radiation. This behavior is observed for all saturated conditions, i.e., for $u_0\geqslant 1$. Note that the absence of unsaturated screening solitons depends on the values of α and β, which in turn depend also on crystal parameters. For our description of SBN, in long propagation conditions *no Kerr regime exists*, a picture that fits well with what is already known (although sometimes attributed to Kerr bulk instability). However, comparing with the effects of Raman shift [15,16], it is possible that, even with the elevated values of E_0 required to self-trap unsaturated solitons, an appropriate crystal (in a given temperature region) may be found with considerably low values of β such as to allow a quasi-Kerr nonlinearity.

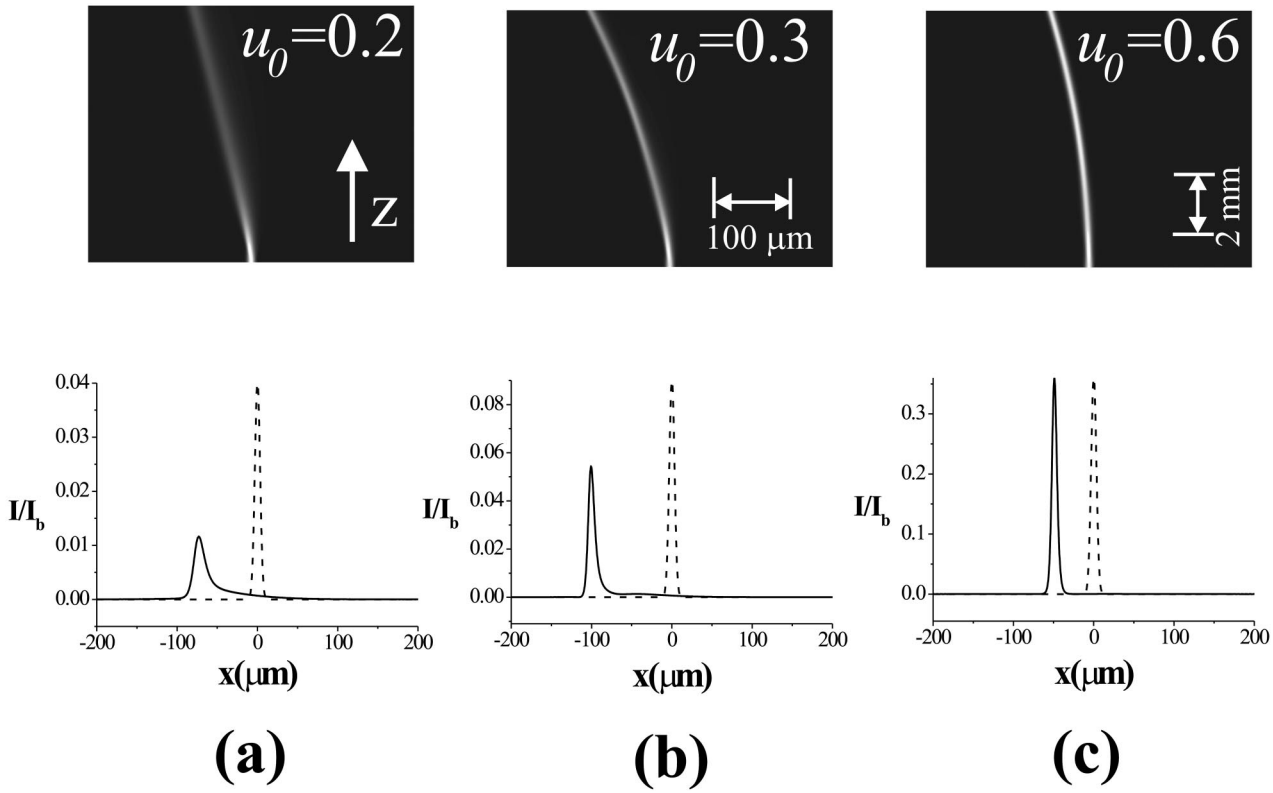

FIG. 1. Transition to a solitonic propagation from unsaturated conditions (a) and (b), for which the $\Delta x=7$-μm beam does not self-trap for any value of E_0. The onset of self-trapping occurs at approximately $u_0 \simeq 0.6$, for which an $E_0=4.2$ kV/cm traps the beam along the $L_z=9.6$-mm propagation ($\gamma=15$) (c). Top row are the respective top views of the intensity distribution, bottom row are the input (dashed line) and output (solid line) intensity profiles.

The first intriguing circumstance appears when we extend our studies to find the existence conditions of self-trapped (and, of course bending) beams. The surprising result is that, in saturated conditions, the corresponding existence curve, in the $(u_0, \Delta\xi)$ plane, hardly varies changing, and for example increasing, γ. More importantly, it is almost unvaried with respect to the existence curve of the *local* treatment [11], for which α and β are artificially set to zero. For example, in Fig. 2(a), numerical results attained with the shooting technique [using the ordinary nonlinear Eq. (4) introduced below] for a $\gamma \simeq 13$ indicate that nonlocal effects apparently do *not* influence existence conditions, as observed in experiments [17]. Note that this does not occur because the nonlocal components play no role. In fact, these make the beam follow a parabolic trajectory (as discussed below), whose respective values of curvature $B=x_s/L_z^2$, x_s being the beam lateral shift at the output, are shown in Fig. 2(b).

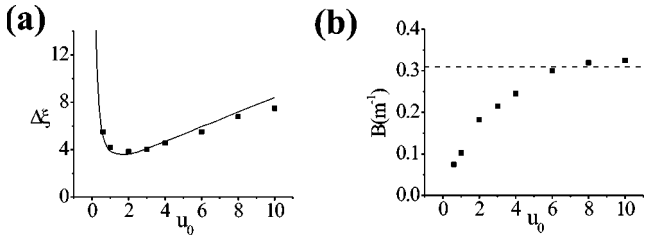

FIG. 2. Invariance of existence conditions even for a long propagation regime of $\gamma=13$, for a $\Delta x=12$-μm beam propagating in a $L_z=20$-mm sample (squares) with respect to the local existence curve (line) (a); validity of the analytical prediction for $B(u_0 \gg 1)$ (b).

To understand this behavior we follow the established solitonic analysis by self-consistently imposing a symmetry to the system on consequence of propagation invariance, reducing the nonlinear Eq. (3) to an ordinary differential equation. The built-in Galileian-like symmetries, originally implemented by Gagnon *et al.* [19] to address soliton self-frequency shift in Kerr-like materials, indicate that the reduction occurs in an *accelerated* transverse frame, as discussed in Ref. [16]. Solitons will thus be of the type $w(\xi,\zeta)=u(\Xi)\exp\{-i\zeta[(b^2/6)\zeta^2-(b/2)\xi+q]\}$, where u is real, $\Xi=\xi-(b/2)\zeta^2$, and q and b are matching parameters. For a local nonlinearity, the transformation is limited to a frame with zero acceleration, i.e., with $b=0$, leading to the standard condition $w(\xi,\zeta)=e^{-iq\zeta}u(\xi)$. The transformation does *not a priori* imply that solitons form [16,20,21].

Implementing the transformation, the ordinary nonlinear equation

$$u_{\Xi,\Xi}+qu-\left(\frac{b}{2}\right)\Xi u-\frac{u}{1+u^2}+\alpha\frac{u^2u_{\Xi}}{1+u^2}+\beta\frac{u^2u_{\Xi}}{(1+u^2)^3}=0 \tag{4}$$

is obtained, where subscripts identify derivatives. A first straightforward observation is that the transformation intro-

duces a characteristic linear transverse phase chirp $-(b/2)\Xi u$. Considering, for the moment, only charge diffusion [i.e., $\beta=0$ in Eq. (4)], the nonlocal term, for the saturated (i.e., $u_0 \gg 1$) regime, can be approximated to $\alpha u^2 u_\Xi/(1+u^2) \simeq \alpha u_\Xi$. Apart from beam tails, the soliton bell shaped structure is a quasi-Gaussian (see, for example, Ref. [22]), and $u \simeq u_0 \exp(-\Xi^2/\Xi_0^2)$ (Ξ_0 deriving from Δx), with $u_\Xi \simeq -(2\Xi/\Xi_0^2)u$. Approximations are warranted by the fact that the term is a corrective $o(\eta)$. Thus Eq. (4) manifests a property which results particularly enlightening. The nonlocal part gives approximately itself a linear phase chirp: exactly the result of the symmetry transformation. Thus, if we choose to describe the beam in the system in which $b=-4\alpha/\Xi_0^2$, the nonlinear propagation equation reduces to

$$u_{\Xi,\Xi} + qu - \frac{u}{1+u^2} = 0, \tag{5}$$

which is none other than the screening equation obtained by fully neglecting the nonlocal components [11].

This at once forwards an explanation to the existence-condition invariance illustrated in Fig. 2(a), which, however, must be tested (as usual, the soliton prediction is self-consistent). If the reasoning is physically sound, we have an *analytical* approximation to the actual soliton trajectory which can be quantitatively tested against numerical findings. In Fig. 2(b) the calculated asymptotic parabolic curvature $B(u_0 \gg 1)=n^2 r k_b T/(\omega_0^2 q)$, where ω_0 is the beam width **(**i.e., $\Delta x=[2\ln(2)]^{1/2}\omega_0$**)**, is compared with simulation results. The good agreement forms the confirmation of our reasoning.

The approximate treatment indicates that the leading term in the new description of the self-bent beam supports a soliton, with its propagation invariance *and* its particlelike manifestations. Moreover, it is *the very same soliton that would appear in the absence of nonlocal processes, with the very same existence conditions*, albeit along a parabolic trajectory.

Therefore we find the exact opposite to an intrinsic limitation in long propagation solitonic regimes: in conditions in which solitons emerge, *the full nonlinearity is actually local*. The soliton, to form, follows that trajectory that allows for this circumstance, i.e., that for which the system of reference is transformed so as to allow for a saturated Kerr manifestation. In this we identify the intrinsically "local" nature of photorefractive solitons, clarifying the peculiarity observed in experiments and detailed in the numerical results. The circumstance is evidently associated to the highly selective (but stable) conditions that lead to *self-trapping*. A different perspective, as for example held in Ref. [12] where the focus is on general beam behavior, sees bending as a further control parameter, which is not rigidly fixed by launch conditions, as instead occurs for solitons. In this case, bending can be implemented for a controllable routing, but it cannot lead to self-trapping, since it implies a *z*-evolving beam. The phenomenon is analogous to self-deflection [23].

Note the physical distinction between beam fanning [24] and bending induced by spatial nonlocality for an extended and, respectively, a confined beam. For the finite size of the propagating soliton, fanning does not intervene (there are no radiating waves), as the absence of relevant scattering, a consequence of Eq. (5), shows. Diffusion, conversely, introduces an approximately linear transverse chirp that rigidly shifts the wave-vector distribution, without altering its shape, such that energy is coupled from the initial modes to different ones that are themselves guided and part of the soliton, which congruently rotates in space. Emblematic of this is the fact that the actual numerical aperture of the soliton beam, which remains unvaried during propagation, influences the value of B, but not the overall beam inclination θ, which scales with L_z. In so much that the prediction transfers to the higher two-plus-one-dimensional soliton case, this fact indicates that a soliton-based circuit, even in a realization that involves long propagation regimes, can be efficiently coupled out from Ref. [25] and back into a fiber-based circuit, the butt coupling being appropriately aligned along the parabola.

The entire reduction from Eq. (4) to Eq. (5) indicates that nonlocality bends the beam trajectory, but, on consequence of saturation, this does not lead to radiation loss or distortion, to the point that even the existence conditions of self-trapping remain *unaltered* from those of a short propagation (unbending) regime. From an intuitive perspective, in the unsaturated limit discussed in Refs. [15,16], the induced guiding index of refraction pattern is not capable of capturing all the light in the diffracting beam when the effects of curvature intervene. With an elevated saturation, the more steplike index pattern can trap a wider angular spread, and even though a curvature in the trajectory is present, no light is emitted, as occurs for most macrobends in step-index fiber.

Apart from these basic considerations, the validity of soliton propagation in long propagation regimes allows us to predict a series of interesting and useful phenomena that not only lie yet unobserved, but could have been previously reasoned inaccessible.

A first consequence is on what we can expect of counterpropagating schemes. The incoherent and coherent interaction of counterpropagating waves in a photorefractive material form part of the fundamental phenomenology associated to the field, in the first case leading to transverse instability, in the second, to wave mixing [24]. A different effect has been predicted for counterpropagating solitons [26], which amounts to a delocalized collision that would allow a driven self-alignment of two micron-guided waves. In order for the effect to emerge, a strong solitonic regime is required, and the consequent elevated values of γ lead to self-bending. This translates into an apparent impossibility of superimposing the trajectories, localizing the interaction into a large angle (i.e., elastic) collision. Our results on the underlying symmetry indicate that when self-trapping occurs (and not for the general case described in Ref. [12]), no distortion intervenes along the propagation axis "tagging" the direction of propagation, and, if the two beams are launched so as to lie on the same parabolic trajectory, they will superimpose *throughout*, leading to the predicted nonlocal interaction. A similar condition has been in part inspected by Rotschild *et al.* [27].

The same symmetry is also at the basis of what we can term "soliton cavities." The absence of a propagation direction distortion, a consequence of the validity of Eq. (5),

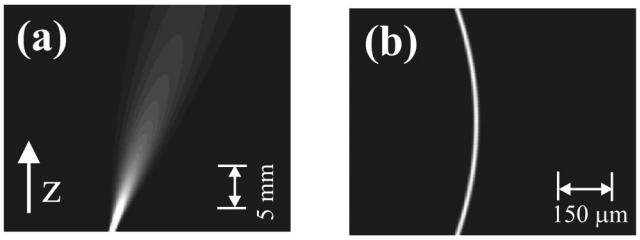

FIG. 3. The highly symmetric formation of a solitonic boomerang for a 29-mm propagation ($\gamma=18$) of a $\Delta x=12$-μm beam, with an initial launch angle $\theta=7.5$ mrad with respect to the z axis. Top view of angled diffraction without applied field (a); and with the trapping $E_0=1.2$ kV/cm ($u_0=4$) (b).

means that these can be achieved by appropriately launching the beam and positioning the reflecting end mirrors. An emblematic basis for a cavity is that illustrated in Fig. 3(b), which represents a "solitonic boomerang," the most symmetric of photorefractive soliton manifestations. By launching a tilted beam, it self-bends and is self-reflected during the trapping process. For a specific tilt and L_z, a given soliton leads to a process which is fully symmetric with respect transverse $z=L_z/2$ plane. A solitonic boomerang could not exist where a propagation distortion were to physically accumulate during propagation. In the example illustrated in Fig. 3(b), the boomerang forms for the $\Delta x=12$-μm beam at $u_0=4$ and input angle $\theta=7.5$ mrad, and an $E_0=1.2$ kV/cm, for a propagation distance of $L_z=29$ mm. The maximum lateral shift of 53 μm is attained half way along the parabolic trajectory.

A second consequence concerns soliton collisions, which form a substantial part of investigated phenomenology [28]. Since interaction depends principally on the relative angle $\theta_r=\theta_1-\theta_2$ between the propagating solitons, self-bending will substantially change the nature of the interaction. Specifically, since the single beams follow parabolic trajectories, θ_r tends to *diminish* along propagation, rendering the saturated event ever less elastic. Only for the case in which the beams are launched parallel this does not occur. As shown in Fig. 4(a), for a launch $\theta_{r0}=0$ the two trajectories are parallel (when the interaction is weak), and tend to remain such. This does not generally correspond to a collision (the beams, however, evolve progressively closer).

For $\theta_{r0}\neq 0$, extended soliton propagation can therefore lead to characteristic events, such as those described in Figs. 4(b) and 4(c), which refer to collisions between solitons in conditions of self-trapping of Fig. 3. The outcome of the collision does not solely depend on θ_{r0} at launch, but also on the intersoliton distance: the larger the distance the farther into propagation the collision occurs, and the lower the relative collision angle θ_c at the point of intersection. The effect is extraneous to a saturated local nonlinearity [see Figs. 4(d) and 4(e)].

The question thus arises as to how we can reproduce "rectilinear" (i.e., $\theta_{r0}\simeq\theta_c$) collisions in photorefractives. Given that the solitons actually form without distortion along a parabola, we can "hop" onto the trajectory along its quasiasymptotic tails, as shown in Fig. 5(a). For a given propagation distance L_z the evolution of θ will be negligible. Thus we can achieve a given value of collision $\theta_{r0}\simeq\theta_c$ (even for large

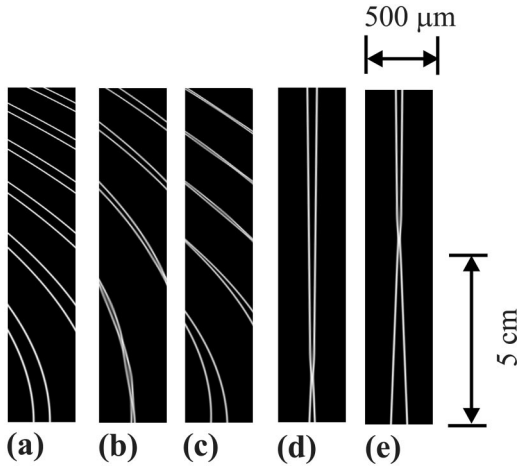

FIG. 4. A collisional anomaly due to bending. For a parallel launch ($\theta_1=\theta_2=0$), the mutually incoherent 12-μm beams, initially 120 μm apart, travel parallel along their parabolic trajectory (a). When $\theta_{r0}=26$ mrad ($\theta_1=-\theta_2$) and the two beams are launched at a distance of 25 μm, the collisional $\theta_c\simeq\theta_{r0}$ results larger than the critical angle that leads to a bound soliton pair (b). If the beams are launched at a distance of 120 μm, the intersection point is farther into propagation, and $\theta_c<\theta_{r0}$, resulting lower than the critical angle: the two beams lock together (c). For a saturated local nonlinearity $\theta_c\simeq\theta_{r0}$ both for a 25-μm (d) and a 120-μm launch (e).

values of γ) by having the two identical solitons hop on in *different* portions of the tails. In Fig. 5 an incoherent (b) [coherent (c)] collision for a local model, in which α and β are artificially set to zero, is compared to the incoherent (d) [coherent (e)] collision for the full model. For the given tail scheme no discernible difference emerges [as instead occurs for the symmetric $\theta_1=-\theta_2$ scheme of Figs. 4(b) and 4(e)].

In some cases, however, the consequences are such as to disrupt some physical mechanism, rendering it inaccessible to observation in the long propagation solitonic limit. A first important class of effects is associated with the self-

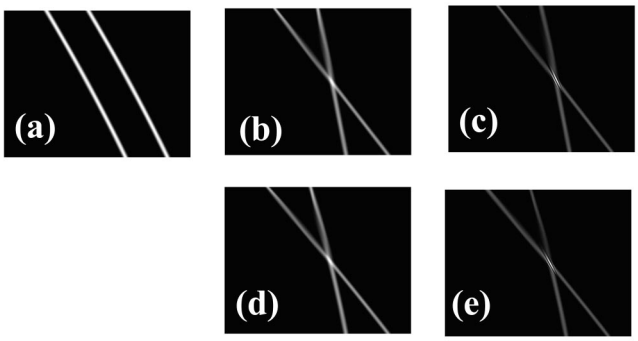

FIG. 5. Quasirectilinear collisions in long propagation regimes of two 7-μm beams with $u_0=4.5$, and trapping field $E_0=3.2$ kV/cm. Parallel $\theta_1=\theta_2=12$-mrad launch, following the *quasiasymptotic* portion of the parabolic trajectory (intersoliton distance 90 μm) (a); comparison between a local saturated incoherent collision for $\theta_1=17$ mrad and $\theta_2=4.3$ mrad (b); a coherent one (c); and, respectively, the same for the photorefractive nonlinearity (d) and (e). No discernible difference emerges along the $L_z=14.4$-mm propagation.

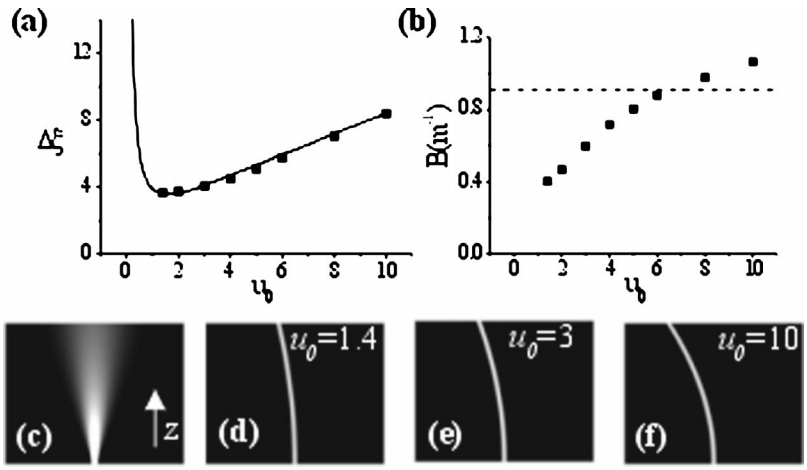

FIG. 6. Invariance of existence curve (a) in conditions of finite charge displacement and breakdown of diffusion based prediction (b). Evidence of self-trapping to a 7-μm soliton of the initially diffracting beam (c) along the L_z=9.6 -mm propagation, in various conditions of saturation (d)–(f). In this case, the condition $E_0^2 \ll k_b T N_a u_0^4/(\varepsilon_0 \varepsilon_r)$ is not fulfilled.

enhancement of electronic nonlinearity: here the intrinsic walkoff must inevitably lead second-harmonic-generation and parametric conversion out of phase matching [8]. Similarly for the interaction of solitons with larger-period structures, where bending can bring the wave into and out of Bragg matching. The condition can once more be mitigated through a tilted scheme [see Fig. 5(a)]. Things are quite different for a soliton array: here *all* the identical solitons self-bend, leading to a rigidly rotating pattern, the basic signature that distinguishes it from interferometrically generated structures. Whereas in the first, the beams propagate independently and accumulate the self-bending chirp, in the second, the interferograms have no propagation, being all coupled by the extended interfering waves, and hence do not suffer self-bending.

All numerical findings take into account the full model of Eq. (4), i.e., both charge diffusion and charge displacement, whereas the basis of our understanding has been attained neglecting the latter. This is a valid assumption for most configurations, such as those illustrated in Figs. 2–4, even for larger values of γ, and holds for all soliton conditions in which $E_0^2 \ll k_b T N_a u_0^4/(\varepsilon_0 \varepsilon_r)$, that in our case translates to $E_0 \ll 1.5 u_0^2$ kV/cm.

In itself, the charge displacement term $\beta u^2 u_\Xi/(1+u^2)^3$ does not directly share the same scaling as the diffusive one: it once again introduces a chirp, but distorted by the $1/Q^2$ factor. One practical manner to slightly enhance its influence is to investigate tighter solitons which, for the same value of u_0^2, leads to an increase of E_0. Results for the Δx=7-μm case are shown in Fig. 6 (the same condition was also implemented in Fig. 1). In particular, the existence curve is still unvaried (a), and self-trapping of the highly diffracting beam (c) follows once again a parabolic trajectory (d)–(f), for different values of u_0. However, in this case, the curvature is due to both terms ($\alpha \neq 0, \beta \neq 0$), and the analytic prediction at the basis of Eq. (5), which allowed the evaluation of bending results in conditions of Fig. 2, leads now to an underestimated value of $B(u_0 \gg 1)$ (b). Concluding, charge displacement does not qualitatively alter our scheme, and is in general a small correction.

A final speculation in this hereto unexplored solitonic regime of long propagation is that the beam trajectory could itself lead, on consequence of the anisotropy of the electro-optic host, to an effective electro-optic coefficient r, and hence a nonlinearity, that changes during propagation, causing a form of nonlinear diffraction. The effect, however, is mitigated by the parabolic form of the trajectory, for which the angle of rotation of the beam $d\theta$ for the propagation from L to $L+dL$ decreases in L according to $d\theta/dL \simeq (1+4B^2L^2)^{-1}$.

By implementing an analytical approximation of the nonlinear propagation equation based on its natural symmetries, we have shown that one-dimensional photorefractive solitons in biased crystals are supported by a local saturable nonlinearity which is a result of both local and nonlocal spatial processes, nonlocality being relegated to determining a nonlinear change in soliton trajectory. This allows the identification of the mechanism that supports soliton formation in the long propagation regime, providing, in some conditions, an explicit analytical prediction of the soliton trajectory and existence points, along with a set of interesting observable effects.

Research was funded by the Italian Istituto Nazionale Fisica della Materia (INFM) through the "Solitons embedded in holograms" (SEH) project, and by the Italian Ministry of Research through the "Space-time effects" Basic Research FIRB project. A.D. acknowledges the support of the DEWS Center for Excellence.

[1] M. Segev *et al.*, Phys. Rev. Lett. **68**, 923 (1992); B. Crosignani *et al.*, J. Opt. Soc. Am. B **10**, 446 (1993); G. C. Duree *et al.*, Phys. Rev. Lett. **71**, 533 (1993); D. N. Christodoulides and M. I. Carvalho, Opt. Lett. **19**, 1714 (1994); S. R. Singh and D. N. Christodoulides, Opt. Commun. **118**, 569 (1995).

[2] M. Segev and G. Stegeman, Phys. Today **51**(8), 42 (1998); G. I. Stegeman and M. Segev, Science **286**, 1518 (1999); *Spatial Solitons*, edited by S. Trillo and W. Torruellas (Springer-

Verlag, Berlin, 2001).
[3] M. F. Shih, M. Segev, and G. Salamo, Phys. Rev. Lett. **78**, 2551 (1997).
[4] M. Mitchell and M. Segev, Nature (London) **387**, 880 (1997).
[5] J. W. Fleischer *et al.*, Phys. Rev. Lett. **90**, 023902 (2003); J. W. Fleischer *et al.*, Nature (London) **422**, 147 (2003); D. Neshev, Opt. Lett. **28**, 710 (2003); M. Petrovic *et al.*, Phys. Rev. E **68**, 055601(R) (2003).
[6] W. Krolikowski and S. A. Holmstrom, Opt. Lett. **22**, 369 (1997); W. Krolikowski *et al.*, *ibid.* **23**, 97 (1998).
[7] J. Petter and C. Denz, Opt. Commun. **188**, 55 (2001); J. Petter *et al.*, Opt. Lett. **28**, 438 (2003).
[8] S. Lan *et al.*, Opt. Lett. **24**, 1145 (1999); S. Lan *et al.*, Appl. Phys. Lett. **77**, 2101 (2000); A. D. Boardman *et al.*, J. Opt. Soc. Am. B **19**, 832 (2002); S. Lan *et al.*, Opt. Lett. **27**, 737 (2002).
[9] E. DelRe *et al.*, Opt. Lett. **25**, 963 (2000); E. DelRe *et al.*, *ibid.* **27**, 2188 (2002).
[10] For example, a $\gamma \simeq 25$ is reported in G. M. Tosi-Beleffi *et al.*, Opt. Lett. **25**, 1538 (2000).
[11] M. Segev *et al.*, Phys. Rev. Lett. **73**, 3211 (1994); M. Segev *et al.*, J. Opt. Soc. Am. B **13**, 706 (1996).
[12] M. I. Carvalho *et al.*, Opt. Commun. **120**, 311 (1995); S. R. Singh *et al.*, *ibid.* **130**, 288 (1996).
[13] Z. M. Sheng *et al.*, J. Opt. Soc. Am. B **13**, 584 (1996); M. I. Carvalho *et al.*, Opt. Commun. **124**, 642 (1996).
[14] J. Petter *et al.*, Opt. Commun. **170**, 291 (1999); C. Denz *et al.*, Phys. Rev. E **60**, 6222 (1999).
[15] N. Akhmediev *et al.*, Opt. Commun. **131**, 260 (1996).
[16] W. Krolikowski *et al.*, Phys. Rev. E **54**, 5761 (1996).
[17] K. Kos *et al.*, Phys. Rev. E **53**, R4330 (1996).
[18] E. DelRe *et al.*, J. Opt. Soc. Am. B **15**, 1469 (1998).
[19] L. Gagnon and P. A. Belanger, Opt. Lett. **15**, 466 (1990).
[20] V. Aleshkevich *et al.*, Opt. Commun. **197**, 445 (2001).
[21] M. Facao and D. F. Parker, Phys. Rev. E **68**, 016610 (2003).
[22] G. Montemezzani and P. Gunter, Opt. Lett. **22**, 451 (1997).
[23] S. Shwartz *et al.*, Opt. Lett. **29**, 760 (2004).
[24] L. Solymar, D. J. Webb, and A. Grunnet-Jepsen, *The Physics and Applications of Photorefractive Materials* (Clarendon, Oxford, 1996).
[25] E. DelRe *et al.*, J. Appl. Phys. **95**, 3822 (2004).
[26] E. DelRe *et al.*, J. Nonlinear Opt. Phys. Mater. **8**, 1 (1999); D. Kip *et al.*, Ferroelectrics **274**, 135 (2002); O. Cohen *et al.*, Phys. Rev. Lett. **89**, 133901 (2002); O. Cohen *et al.*, Opt. Lett. **27**, 2013 (2002).
[27] C. Rotschild *et al.*, J. Opt. Soc. Am. B **21**, 1354 (2004).
[28] M. F. Shih and M. Segev, Opt. Lett. **21**, 1538 (1996); M. F. Shih *et al.*, Appl. Phys. Lett. **69**, 4151 (1996); H. X. Meng *et al.*, Opt. Lett. **22**, 448 (1997); E. DelRe *et al.*, *ibid.* **25**, 560 (2000); J. A. Andrade-Lucio *et al.*, Electron. Lett. **36**, 1403 (2000).